

The Snow Dynamical System for Plant Pattern Formation

Pau Atela and Christophe Golé
Dept. of Mathematics
Smith College

August, 2005

DRAFT FORM

1 Introduction

Plant organs develop at the edge of the growing tip of the plant, called shoot apical meristem. They appear as microscopic bulges of cells called primordia and later grow and differentiate into the different organs (leaves, petals, branches etc...). The regular spacial structure often visible in the grown plant (*e.g.* pineapple, pinecone, sunflower...) is present at the onset of primordia, at a microscopic scale. In [10], the two botanists Snow & Snow posited that primordia form around the apex meristem *when and where* there is enough space left available by the previously formed primordia. This contrasts with Hofmeister's hypothesis (that we studied in [1]) where primordia are constrained to appear at fixed intervals of time.

Other authors have studied models based on the Snow hypothesis ([6], [5], [8]). We choose to implement the principle of the Snows with a simple model which enables us to extract important geometric structures underlying phyllotaxis. The assumptions we make are of a cylindrical meristem border and of circular primordia that only "feel" their nearest neighbors. One of the main feature of this model is that it produces, apart from the usual Fibonacci lattices, periodic configurations: patterns that look like lattices, each with two sets of parastichies, but are not lattices. Note that we had also found periodic patterns in the Hofmeister model [1], but they were isolated. Here periodic configurations come in large families, which are part of a large geometric structure that we call the skeleton. The skeleton also contains the usual lattices of phyllotaxis. The skeleton might provide an explanation of the mysterious speed at which plants stabilize in regular patterns with high parastichy numbers: less precision (and thus less iteration) is needed if the target set of patterns, previously thought to only consist of lattices, is enlarged to that of periodic configurations with same parastichy numbers. Our model is highly idealized, but we conjecture that similar skeletons exist in many other systems (as invariant manifolds) and that the topology of these skeletons organizes the transitions between the different phyllotactic patterns.

A crucial concept in this paper, intimately tied to that of the skeleton is that of "growth front": roughly, the most recent layer of primordia at a given stage of the growth. A growth front determines the future of a pattern that contains it. Thus deforming growth fronts provides a parameterization for the skeleton and a handle into the connections between its different "limbs". We show that when defined, parastichy numbers can be read off the growth fronts. Growth fronts also provide a geometric key to transitions between phyllotactic patterns. As a bonus, growth fronts may provide

an explanation for the frequent presence of Fibonacci number of ray florets in the inflorescence of certain species of plants [3].

We have deliberately set aside many mathematical proofs and computations in this article, to make it readable by a larger audience. Subsequent publications will include them.

2 The Snow Model

We represent the region bordering the apex meristem by a cylinder of unit circumference, which we show unrolled in the pictures of this paper. We also assume that primordia are represented as disks of same diameter D (this is a parameter in the model). We let the upper edge of the cylinder move up and place a new primordium where and when there is room for it between the existing primordia and the upper edge of the cylinder. There may be room for several primordia simultaneously (this will be the case in whorl configurations, see Figure 2). In this case we choose to place them one by one, from left to right, starting at the latest primordium. The ability of this model to produce whorls is its main difference with the Hofmeister model. For mathematical consistency, we consider a fixed number N of primordia at each step and remove one in the bottom to keep that number constant. In the graphics we choose not to remove the bottom primordium. This model is formalized as a discrete dynamical system, see Section 7.

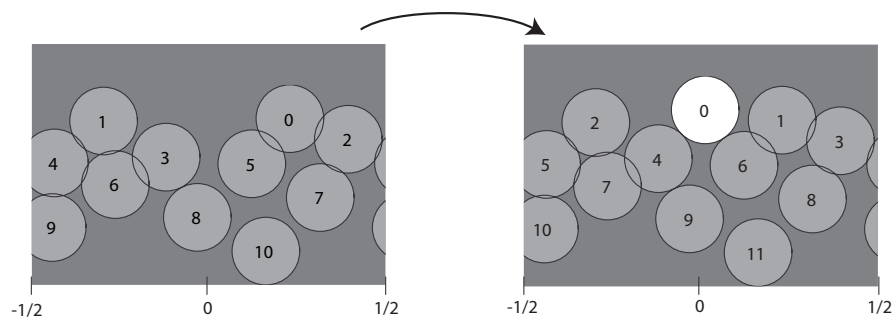


Figure 1: **The Snow map S .** The map S acts on arbitrary configuration of points in the cylinder of circumference 1, represented as unrolled here. Given an initial configuration of points (left), the Snow map places points one by one, where and when there is enough space. As time passes, the upper edge of the cylinder (representing the edge of the apex) moves up. We interpret "enough space" as meaning space enough for a disk of a certain fixed threshold diameter D to fit under the upper edge. To the left, some initial configuration of points, surrounded by disk of diameter D . To the right, the configuration resulting from applying the Snow map. The new primordium is white.

2.1 Snow Model and Growth Fronts

The dynamical rule of primordia formation described above has the following simple geometric consequences on the placement of the new primordium:

1. *Tangency to nearest neighbors.* The new primordium is tangent to its nearest neighbours. There generally are 2 nearest neighbors below it, and in rarer cases, there might be 3 or even

4, but never more.

2. *Equidistance to nearest neighbors.* The new primordium is equidistant to its nearest neighbors. This is a consequence of Item 1 and of the fact that primordia are modeled by disks of same radius
3. *Opposedness of nearest neighbors.* In the generic case, the new primordium is tangent to only two anterior primordia. In this case the centers of these two anterior primordia must lay on opposite sides of a vertical line through the center of the new one. If it were not the case, there would be a possible location adjacent to the one considered for the new primordium that would be lower, and the primordium would have appeared there at an anterior time.

After at most N iterates, all primordia in the configuration (of N) will have been formed following these rules: each one will have two (and in rare cases 3 or 4) “parent” primordia below it and equidistant to it, one on either side. Moreover, after a while, the new primordium will appear in such a way that it is higher (or at least at equal height) than any of the existing primordia. we call the upper layer of such configurations a growth front. The set of line segments joining the centers of adjacent primordia in a growth front form a piecewise linear graph over the x-axis. We believe that the notion of growth front is a powerful and flexible tool to organize all phyllotactic patterns. In particular, will show that the growth front of a phyllotactic lattice (see below) contains all the information about this lattice. We will call *skeleton* the set of all configurations of N primordia that starts from a growth front. The skeleton is topologically identical to the set of all growth fronts, and constitutes an attractor for the Snow dynamical system. Understanding the topology of the skeleton will provide clue as to the transitions between the different phyllotactic patterns observed in nature. We will see more about geometric properties of growth fronts below.

3 Classical Phyllotaxis

3.1 Lattices and Fibonacci Phyllotaxis

One of the most celebrated phenomenon observed in Phyllotaxis is the occurrence of families of spirals (or helixes in the cylinder model studied here) whose numbers follow the Fibonacci sequence. In this model and in the Hofmeister model [1], Fibonacci phyllotaxis configurations are special *cylindrical lattices*. A cylinder lattice can be obtained by placing primordia one at a time, at constant angular and height increments (x, y) along the cylinder (see Figure 2). If one were to use the cylinder as a printing press and rolled it out on a plane, the successive primordia of a cylindrical lattice would appear as part of a straight line (which, rolled back on the cylinder, is called the generative helix). There are also other helixes that are usually more visible in lattices: those going through nearest neighbors. These are called *parastichies*, and they are the ones that often come in pairs of Fibonacci numbers in plants.

A simple argument, identical to that in [1] shows that only cylindrical lattices can be invariant under S . By an *invariant configuration*, we mean here that the last N primordia of the configuration can be exactly superimposed with the last N primordia of its successor (or image under S) in the dynamical process ¹. Not all cylindrical lattices are invariant under the Snow transformation however. Truncate the lattice by taking all the points that are under a certain height. Then add a

¹Mathematically speaking, these configurations are fixed points for the dynamical system S^* obtained from S by “moding out” the translations.

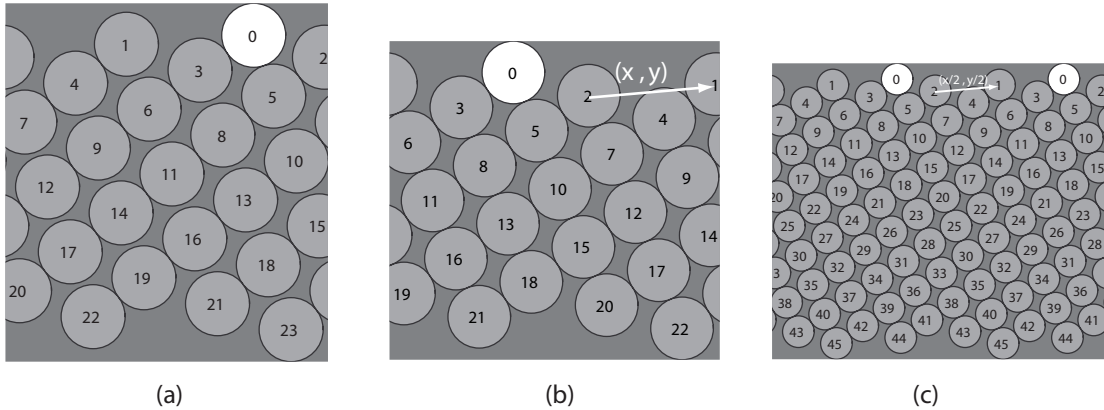


Figure 2: **Cylindrical Lattice and k-jugate configurations.** (a) This cylindrical lattice is not fixed under the transformation S : it does not satisfy the equidistance rule and thus the new primordium does not continue the pattern of the lattice. (b) This cylindrical lattice is fixed under S . The increment vector (x, y) is shown in white. (c) This is a 2-jugate (also called bijugate) configuration obtained by taking two copies of the lattice in (b), scaling them by $1/2$ and placing them at distance $1/2$ along the horizontal axis from one another. Both lattices in (a) and (b) have parastichy numbers 3 and 5. One can follow a parastichy along $\{0, 3, 6, 9 \dots\}$. There is a total of 3 parastichies parallel to this one. Likewise there are 5 parastichies parallel to $\{0, 5, 10, \dots\}$ (including it). The configuration in (c) has parastichy numbers 6 and 10, also denoted $2(3,5)$. It is preserved under two iterations of S .

primordium to that part of the lattice according to the transformation S . If the new primordium is part of the original lattice, such a lattice is preserved and we call it *fixed lattice configuration* of the transformation S . The simple geometric rules of Section 2.1 impose constraints on fixed lattice configurations. These were worked out in this context (configurations of tangent disks) by [5]. A thorough analysis appears in [1]. This analysis yields a bifurcation diagram (Figure 3) that classifies all possible lattices that are fixed under S for all possible values of the parameter D . It also explains the predominance of the fixed points with number of parastichies that are successors in the Fibonacci sequence. We emphasize here that, since this analysis was entirely based on the same three rules spelled out in Section 2.1, the Snow model considered here affords the exact same bifurcation diagram as that of [1].

3.2 Multijugate Configurations

Other configurations preserved by S (but not by the Hofmeister model) are *multijugate* or, more precisely, *k-jugate configurations*. A *k-jugate* configuration can be seen as a lattice together with k of its translates equally spaced along the horizontal axis (see Figure 2, (c)). It is easy to verify that if the lattice with angular and vertical increment (x, y) is a fixed point of S for a value D of the parameter, then the *k-jugate* configuration consisting of k copies of the lattice with increments $(x/k, y/k)$ is fixed by S^k (k consecutive iterates of S) for the value D/k of the parameter. Thus the bifurcation diagram for *k-jugate* configurations consists of k copies of the fixed point bifurcation diagram, rescaled by a factor of $1/k$ and set side by side. In nature, one detects *k-jugate* configurations when the parastichy numbers have a common divisor. And again, the *k-jugate* bifurcation diagram explains why multiples of Fibonacci numbers are predominant

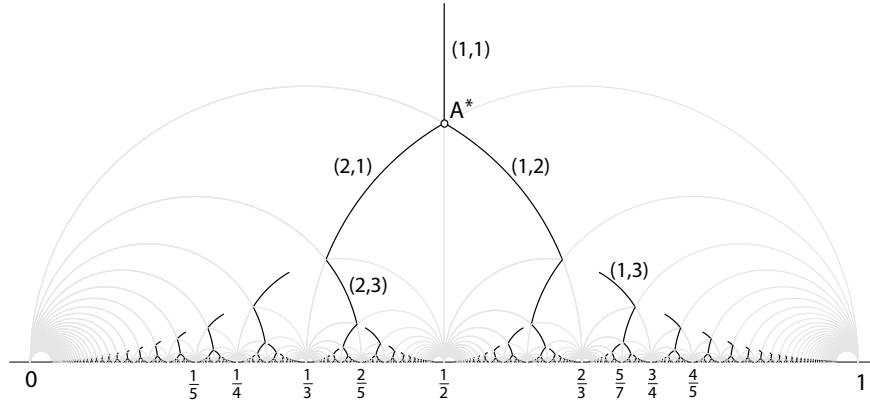


Figure 3: The fixed point bifurcation diagram of the transformation S . The x -axis is the angular increment and the y -axis represents the vertical increment between successive points in the corresponding lattice. Hence a point (x, y) in this plane represents a unique cylindrical lattice. The branches (in black) of the diagram represent the lattices that are fixed lattice configurations. Going down a branch, one travels through regions where the pairs of parastichy numbers for the lattices follow Fibonacci-like sequences: $(m, n) \rightarrow (m + n, n)$. As clearly shown in the diagram, the predominant branches are those starting with $(m, n) = (1, 1)$, yielding the Fibonacci sequence proper. These branches converge to the Golden angle and its complement. Note that the parameter D decreases with y .

among k -jugate configurations in plant Phyllotaxis (the sequence $(2, 6)$, $(6, 10)$, $(10, 16)$... with $k = 2$ is particularly common).

4 New Phenomena

4.1 Periodic Configurations

The most striking phenomenon observed with the Snow model presented here is that most configurations converge in finite time to periodic configurations in the skeleton. These configurations have patterns repeating periodically (up to a rotation of the cylinder). This is best seen through what we will call here *growth fronts*. Applying S for a sufficient number of times on any configuration, primordia will form a barrier between the top and the bottom of the cylinder (the configuration will "hold water if you pour it on top"). In this case, we define the growth front to be the top layer of primordia, *i.e.* the set of primordia that are accessible from the top at a given time. These growth fronts can be visualized at each iterate of S in a configuration, and each one entirely determines the future history of the configuration. Figure 4 (a) shows how periodicity can be visualized through successive growth fronts: the same front reappears periodically, translated by a fixed vector. Mathematically, a periodic configuration of period p can be seen as the union of p copies of the same lattice translated in the plane by different vectors. Such sets are sometimes called *multilattices*. Multijugate configurations are special cases of multilattices, all of whose translation vectors are horizontal. The same way that not all lattices can be generated by S , not all multiple lattices form part of the skeleton of S . But numerical evidence indicates that most of the skeleton is made of multiple lattices, *i.e.* periodic configurations.

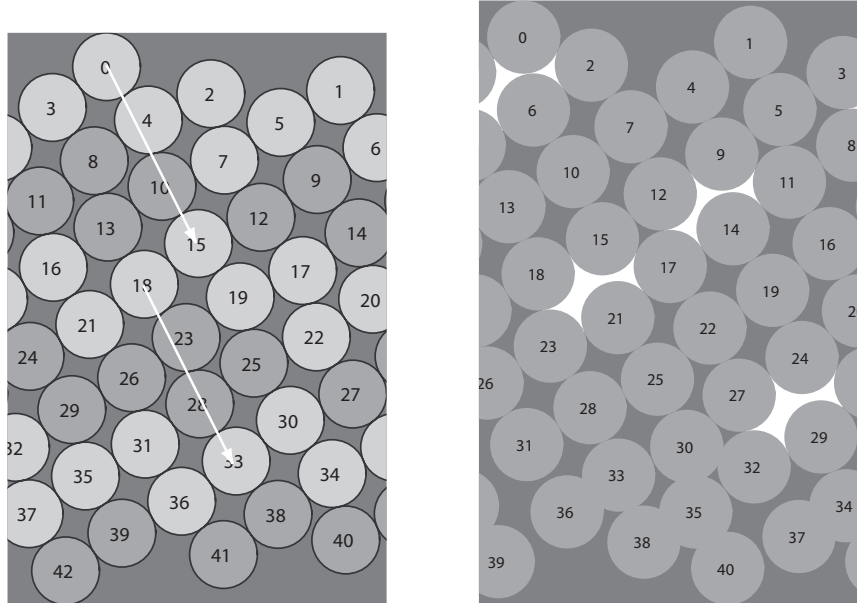


Figure 4: **(a) Period 15 Configuration** (a) This configuration was obtained by iterating the transformation S on a perturbation of the 3,5 fixed point lattice of Figure 2 b. The periodicity of this configuration is underlined here by the lighter shading of “growth fronts”. One can see (and prove) that these growth fronts are translates of one another. The translation vector (shown in white) joins primordium 0 to primordium 15, and, in general, i to $i + 15$. Note also that this configuration has 3 undulating parastichies, winding one way, 5 the other way. **(b) Asymptotically periodic orbit, with pentagons** Experiments show that the majority of orbits settle into a periodic configuration as in (a) in *finite time*. Others do so asymptotically, as in this example. The mechanism seems to always involve sequences of “pentagons” (shown in white) whose width decreases exponentially. Note that the limit configuration will have primordia tangent to three below.

4.2 Finite time vs. Asymptotic Convergence to Periodic

Our numerical studies indicate that the majority of configurations settle into some periodic configuration in finite time. Section 7 sheds some light on the predominance of this behavior. The remaining configurations that we have observed show an interesting phenomenon that needs to be studied further: they also tend to periodic configurations, but apparently in infinite time. The barrier to locking into a periodic configuration in finite time seems to come from the presence of “pentagons”: an interspace bordered by five primordia. In each case we have observed, these pentagons are eventually arranged periodically along the configuration, with their width tending to zero exponentially. In very rare cases we have observed isolated hexagons as well.

5 A Sufficient Condition for Periodicity

In the previous section, we pointed out that pentagons seem to prevent periodicity. In this section, we will argue that “quadrilateral” interspaces between primordia eventually guarantee periodicity. To make this statement more precise, note that most primordia are tangent to two “parent” pri-

mordia below them (more rarely there will be 3 or even 4 such primordia). Assume this is the case for primordium i . Call $L(i)$ and $R(i)$ the left parent and right parent of i respectively. These two parent primordia have themselves parents that we can denote by $LL(i), RL(i), RR(i), LR(i)$.

Theorem 1. *If each primordia has exactly two parents and if the condition $RL(i) = LR(i)$ is satisfied for all primordium i , the configuration is periodic*

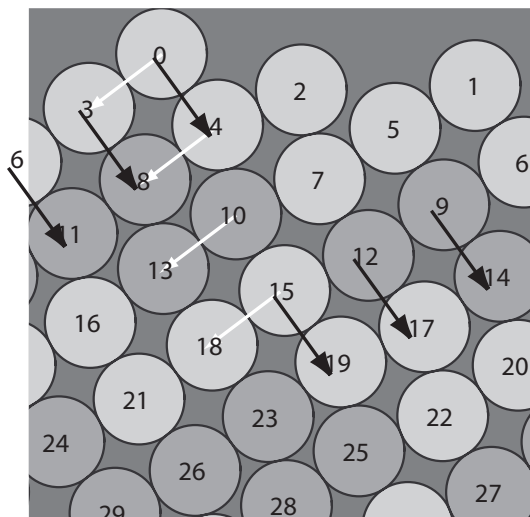


Figure 5: **RL=LR implies periodicity.** Starting at primordium 0, the left parastichy $LP(0) = \{0, 3, 6, \dots\}$ and right parastichy $RP(0) = \{0, 4, 10, \dots\}$ cross at primordium 15. We claim that the configuration has period 15. The condition $RL=LR$ implies that the quadrilaterals enclosed by adjacent primordia are all parallelograms. Hence the white vectors in the picture are all the same, and the black vectors are all the same. This means that the group of three primordia $\{15, 18, 19\}$ has the same shape as the group $\{0, 3, 4\}$ (it is a translate of it by the vector $V_{0,15}$). Extending this reasoning shows that the growth front culminating at 15 is the translate of the growth front culminating at 0. Likewise, any growth front in this configuration reappears periodically, with same period and translation vector as the one singled out here.

We give an idea of the proof, which is illustrated by Figure 5. Note first that $RL(i) = LR(i)$ implies that the center of primordia $i, R(i), L(i)$ and $RL(i)$ are the vertices of a quadrilateral, which must be a parallelogram since all primordia have same radius. By following the left "ancestors" of a primordium i , one obtains a string of primordia tangent to one another. Call this string the *left parastichy*, and denote it by $LP(i)$. This parastichy heads down and left from i . Define the right parastichy $RP(i)$ similarly. These two parastichies must intersect at another primordium $i+k$ below². We claim the configuration is of period k , that is, translating the configuration by the vector $V_{i,i+k}$ which joins the centers of primordia i and $i+k$ does not change the configuration. We refer to Figure 5 and its caption for a graphical argument of this fact.

²One can discard the case where $LP(i)$ and $RP(i)$ are asymptotically vertical: the space between these two verticals would have been filled by primordia some of which would have to be part of these parastichies.

6 Growth Fronts, Parastichy Numbers and Transitions

6.1 Parastichy Numbers and Period

I think this paragraph needs reworking. It could be simple, but it is also fundamental.

Given a periodic configuration which satisfies $RL = LR$, we saw in the previous section that right and left parastichies could be defined through each primordia. The relation $RL = LR$ implies that left parastichies are parallel in a loose sense: the left parastichies through two different primordia either intersect or coincide. The same is obviously true for right parastichies. Thus, as with lattices, we can define parastichy numbers (m, n) as the number of distinct left and right parastichies respectively.

Theorem 2. *Let (m, n) be the parastichy numbers of a periodic configuration which satisfies $LR=RL$. Then:*

1. *The period of the configuration is mn .*
2. *The number of primordia in any growth front of the configuration is $m + n$.*
3. *The number of primordia going down as one travels along a growth front from left to right is m , the number of primordia going up is n*

Hence we can read off the parastichy numbers from the the growth front. Note that Item (2) might be an explanation of why many inflorescence which have Fibonacci phyllotaxis also have a Fibonacci number of petals or ray florets: it would make sense that petals would stem from a single growth front of the growing plant. In this case, the number of petals would equal the sum of the parastichy numbers. This is a Fibonacci number, as it is the sum of two consecutive Fibonacci numbers. Note that a fixed point lattice of parastichy numbers m, n is periodic of period 1 as well as mn . Hence Theorem 6.1 applies to fixed point lattices in particular.

We now give the simple geometric ideas for the proof of Theorem 6.1 through an example. In Figure 5, consider the “necklace” formed by taking the left and right parastichies at 0, $LP(0)$ and $RP(0)$ in our notation) and cutting them below 15. This necklace includes, going from left to right, primordia 4, 10, 15 (going down $RP(0)$) and 12, 9, 6, 3, 0 going up $LP(0)$). It is not a coincidence that the number of “down” primordia is equal to 3, the number of left parastichies here: $LP(4)$ cannot equal $LP(0)$ since 4 is in $RP(0)$ and 15 is the first primordium which is in both $LP(0)$ and $RP(0)$. Likewise $LP(10) \neq LP(0)$. The same argument explains why the number of up primordia in the necklace is equal to 5, which is the number of distinct right parastichies.

Consider now the string of the necklace, made of the vectors $V_{0,4}, V_{4,10}, V_{10,15}$ (going down), $V_{10,15}, V_{15,12}, V_{12,9}, V_{9,6}, V_{6,0}$ (going up). Clearly “up” or “down” quality of each of these vectors reflects the same quality of the primordium at its tip. Consider now the vectors forming the string of the growth front. We claim that these vectors are the same as those in the necklace: $V_{4,2} = V_{15,12}, V_{2,7} = V_{4,10}, \dots$ etc. and this correspondence is one to one. Here is how we build this correspondence: take two consecutive primordia i, j in the growth front, suppose that $V_{i,j}$ is a down vector, so that j is in $RP(i)$. If both i, j are already in the necklace, we are done (*e.g.* 0 and 4). If not $RP(i) \neq RP(0)$ but we can translate $V_{i,j}$ along $LP(i)$ until $LP(i)$ meets $RP(0)$. Because of $LR = RL$ the translated vector must be in $RP(0)$. In the example, translating $V_{2,7}$ along $LP(2)$ gives $V_{4,10}$.

6.2 Transitions

Since parastichy numbers can be read off growth fronts, it is not surprising that growth fronts may also hold the key to transitions between different phyllotactic patterns. Transitions will occur when, deforming a growth front, one reaches a growth front yielding a *triple tangency*, that is when a new primordium rests on 3 older ones instead of the normal 2. This has the effect of changing the length of the growth front by 1, and thus, from what we saw in the previous section, it also changes one of the parastichy numbers by 1. The deformation of growth fronts occurs naturally as the parameter D varies during the growth.

Evidence for this phenomenon actually occurring in nature can be readily gathered on many pineapples, where often, a parastichy is seen to split in two, thus disturbing the usual parastichy numbers of 8, 13 by 1. This phenomenon is called *dislocation* in crystallography and also by the botanist Zagorska-Marek [11], where the author suggests that dislocations are the key to phyllotactic transitions.

Note also that, for configurations with pentagons, there is a change of 1 in the number of primordia in the limit (where pentagons collapse). This is visible in Figure 4, where the growth fronts have 7 primordia and those of the limiting configuration have 8.

In a more well known phenomenon, note that the transition from m, n to $n, m + n$ in Fibonacci phyllotaxis in the present model (as well as in our Hofmeister model [1]) occurs at configurations that are hexagonal lattices. In such lattices, *all* primordia are tangent to three older primordia below them. Interestingly, in their study of their Snow models, Douady and Couder [6] find the transition from 2,3 to 3,3 (whorls) to occur close to the transition 2,3 to 3, 5. In our numerical studies, we have found many 3,3 periodic orbits near that transition point as well.

6.3 Families of Periodic Configurations

Consider a periodic configuration which satisfies the commutativity condition $RL(i) = LR(i)$. By definition this configuration is in the skeleton (see Section 2.1). The future of this configuration is entirely determined by any one of its growth fronts. It is clear that in most cases, any small distortion of a growth front (while maintaining the tangency relations within its primordia) yields a configuration that is still commutative, and thus periodic by Theorem 1 (and still in the skeleton). This perturbation argument shows that the skeleton contains continuous families of periodic orbits – a fact that is supported by our numerical simulations.

Moreover, growth fronts give us the number of free parameters needed to describe all such distortions, and hence the dimension of the families of periodic configurations we may obtain around a given one. Indeed, a growth front is determined by the position of one of its primordia and the angles between adjacent pairs of primordia in the growth front. If the growth front has L primordia then there are L angles. Since the last two angles are determined by the other $L - 2$ (placing $L - 1$ primordia in the front determines the placement of the last), the space of all periodic configurations around a particular one is of dimension L ($L - 2$ angles and the 2 coordinates of one primordium. Note that the dimension of a space is the number of free variables necessary to describe it). In the example of Figure 5, a growth front has length $L = 8$ so the space of period 15 configurations around this particular one is of dimension 8. The same argument shows that the space of periodic configurations surrounding a periodic configuration of parastichy numbers m, n is of dimension $m + n$. Note that this dimension drops by 2 if we are only interested in the shape of the configuration, not its exact location in the cylinder (mathematically, we would be moding out by translations).

7 Stability

In this more mathematical section, we show that fixed point lattices are stable, but are not attractors, as was the case in the Hofmeister model [1]: configurations close to a fixed point lattice will stay close but will not converge to it. This relatively “bad news” is alleviated by the following: in the families of Snow models studied by Douady and Couder [6], fixed points lattices are attractors. The model studied here is an asymptotic limit of Douady and Couder’s models, when a certain parameter is varied (“hardness of disks”). We plan to perform an asymptotic analysis to prove this stability rigorously.

We also conjecture that large parts of the skeleton of the map S survives under perturbations of the map itself, in the guise of invariant manifolds for finite iterates of the perturbed map. Namely the configurations on these perturbed surfaces may not be periodic any more, but they will be close to our periodic orbits. We conjecture that transitions between different patterns will occur along these surfaces, hence the importance of studying them.

We now make the set up of our model more precise mathematically (more details will be given in a future publication). The space on which the map S acts is parameterized by

$$\{(x_0, y_0), (x_1, y_1), \dots, (x_{N-1}, y_{N-1})\}$$

where (x_i, y_i) are the coordinates of the i^{th} primordium in a configuration of N primordia. The number N can be arbitrarily large, and in practice we choose it to be larger than the size of the longest possible growth front possible for the given parameter D . The space is thus the cartesian product of N cylinders, or, equivalently the product $\mathbb{T}^N \times \mathbb{R}^N$ of the N -torus by the N -Euclidean space. The map S is of the form:

$$S\{(x_0, y_0), (x_1, y_1), \dots, (x_{N-1}, y_{N-1})\} = \{(X_0, Y_0), (X_1, Y_1), \dots, (X_{N-1}, Y_{N-1})\}$$

where $(X_i, Y_i) = (x_{i-1}, y_{i-1})$ when $i \neq 0$ and (X_0, Y_0) is the position of the new primordium, the center of the lowest disk an algebraic function of its two neighbors. We can show that the characteristic polynomial of the differential of the map at a lattice fixed point is $\lambda^K(1 - \lambda^m)(1 - \lambda^n)$ where m, n are the nearest neighbors to the new primordium, and $K = N - m - n$. Since the roots of this polynomial are either 0 or the m^{th} and n^{th} roots of unity, the fixed point lattices are only linearly stable³. This result is not surprising, in light of the fact that the fixed point is surrounded by periodic orbits in the skeleton: the non zero eigenvalues correspond to eigenspaces tangent to the skeleton, and the zero eigenvalue accounts for the superattractivity of the skeleton.

We conjecture that at least large parts of the skeleton survive when the map S is perturbed slightly. Mathematically, this should be due to the “normal attraction” of the skeleton.

References

- [1] Atela, P., Golé, C. & Hotton, S., A Dynamical System for Plant Pattern Formation: Rigorous Analysis. *J. Nonlinear Sci.* Vol. 12, Number 6 (2002)
- [2] Atela, P. & Golé, C., New Concepts in Phyllotaxis: Primordia Fronts and Multilattices (preprint, 2005)

³We are being a little short here: the fixed point lattices are only fixed points when one factors out the translation symmetry in the system. The quotient map will have same spectrum, except for the double eigenvalue 1, which disappears in the quotient. See [1] for a similar argument.

- [3] Atela, P., Golé and Smith students, *Phyllotaxis: an interactive site for the mathematical study of plant pattern formation* <http://www.math.smith.edu/phylo/>
- [4] Battjes, J. & Prunskiewicz, P. , Modelling Meristic Characters of Asteracean Flowerheads in , *Symmetry in Plants* World Scientific, (1998), pp. 281-312.
- [5] *On the relation of phyllotaxis to mechanical laws*, (1904)
- [6] Douady S., The Selection of Phyllotactic Patterns, *Symmetry in Plants* World Scientific, (1998), pp. 335-358.
- [7] Douady S. & Couder Y., Phyllotaxis as a Self Organizing Iterative Process, Part I, II & III, *J. Theor. Biol.* **178**, (1996), pp. 255-312.
- [8] Hotton, S., *Thesis*, University of California, Santa Cruz (1999).
- [9] Kunz M., *Thèse*, Université de Lausanne, Switzerland (1997).
- [10] Robinson, C., *Dynamical Systems*, CRC Press, (1994).
- [11] Snow M. & Snow R., Minimum Areas and Leaf Determination, *Proc. Roy. Soc.*, **B139**, (1952), pp 545-566.
- [12] Zagórska-Marek B., Phyllotactic Diversity in *Magnolia* Flowers, *Acta Soc. Bot. Poloniae* **63** (1994), pp. 117-137.